

# Hunting for Frozen Super-Earths via Microlensing

Jean-Philippe Beaulieu<sup>1,3</sup>

Michael Albrow<sup>1,4</sup>

Dave Bennett<sup>1,5</sup>

Stéphane Brillant<sup>1,6</sup>

John A. R. Caldwell<sup>1,7</sup>

Johannes J. Calitz<sup>1,8</sup>

Arnaud Cassan<sup>1,9</sup>

Kem H. Cook<sup>1,10</sup>

Christian Coutures<sup>1,3</sup>

Stefan Dieters<sup>1,11</sup>

Martin Dominik<sup>1,2,12,13</sup>

Dijana Dominis-Prestler<sup>1,14</sup>

Jadzia Donatowicz<sup>1,15</sup>

Pascal Fouqué<sup>1,16</sup>

John Greenhill<sup>1,11</sup>

Kym Hill<sup>1,11</sup>

Matie Hoffman<sup>1,8</sup>

Uffe G. Jørgensen<sup>1,17</sup>

Stephen Kane<sup>1,18</sup>

Daniel Kubaš<sup>1,6</sup>

Jean-Baptiste Marquette<sup>1,3</sup>

Ralph Martin<sup>1,19</sup>

Pieter Meintjes<sup>1,8</sup>

John Menzies<sup>1,20</sup>

Karen Pollard<sup>1,4</sup>

Kailash Sahu<sup>1,21</sup>

Christian Vinter<sup>1,17</sup>

Joachim Wambsganss<sup>1,9</sup>

Andrew Williams<sup>1,19</sup>

Kristian Woller<sup>1,17</sup>

Marta Zub<sup>1,9</sup>

Keith Horne<sup>1,2,12</sup>

Alasdair Allan<sup>2,22</sup>

Mike Bode<sup>2,23</sup>

Daniel M. Bramich<sup>1,2,24</sup>

Martin Burgdorf<sup>2,23</sup>

Stephen Fraser<sup>2,23</sup>

Chris Mottram<sup>2,23</sup>

Nicholas Rattenbury<sup>2,25</sup>

Colin Snodgrass<sup>2,6</sup>

Iain Steele<sup>2,23</sup>

Yiannis Tsapras<sup>2,23</sup>

<sup>1</sup> PLANET Collaboration

<sup>2</sup> RoboNet Collaboration

<sup>3</sup> Institut d'Astrophysique de Paris, CNRS, Université Pierre et Marie Curie, Paris, France

<sup>4</sup> University of Canterbury, Department of Physics and Astronomy, Christchurch, New Zealand

<sup>5</sup> University of Notre Dame, Department of Physics, Notre Dame, Indiana, USA

<sup>6</sup> ESO

<sup>7</sup> McDonald Observatory, Fort Davis, Texas, USA

<sup>8</sup> Boyden Observatory, University of the Free State, Department of Physics, Bloemfontein, South Africa

<sup>9</sup> Astronomisches Rechen-Institut (ARI), Zentrum für Astronomie, Universität Heidelberg, Germany

<sup>10</sup> Lawrence Livermore National Laboratory, Livermore, California, USA

<sup>11</sup> University of Tasmania, School of Mathematics and Physics, Hobart, Tasmania, Australia

<sup>12</sup> Scottish Universities Physics Alliance, University of St Andrews, School of Physics and Astronomy, St Andrews, United Kingdom

<sup>13</sup> Royal Society University Research Fellow

<sup>14</sup> University of Rijeka, Physics Department, Faculty of Arts and Sciences, Rijeka, Croatia

<sup>15</sup> Technische Universität Wien, Austria

<sup>16</sup> Observatoire Midi-Pyrénées, Laboratoire d'Astrophysique, Université Paul Sabatier, Toulouse, France

<sup>17</sup> Niels Bohr Institutet, Astronomisk Observatorium, København, Denmark

<sup>18</sup> Department of Astronomy, University of Florida, Gainesville, Florida, USA

<sup>19</sup> Perth Observatory, Perth, Australia

<sup>20</sup> South African Astronomical Observatory

<sup>21</sup> Space Telescope Science Institute, Baltimore, Maryland, USA

<sup>22</sup> eSTAR Project, School of Physics, University of Exeter, Devon, United Kingdom

<sup>23</sup> Astrophysics Research Institute, Liverpool John Moores University, Birkenhead, United Kingdom

<sup>24</sup> The Isaac Newton Group of Telescopes, Santa Cruz de La Palma, Canary Islands

<sup>25</sup> The University of Manchester, Jodrell Bank Observatory, Macclesfield, Cheshire, United Kingdom

In order to obtain a census of planets with masses in the range of Earth to Jupiter, eight telescopes are being used by the combined microlensing campaign of the PLANET and RoboNet collaborations for high-cadence photometric round-the-clock follow-up of ongoing events, alerted by the OGLE and MOA surveys. In 2005 we detected a planet of 5.5 Earth masses at 2.6 AU from its parent 0.22  $M_{\odot}$  M star. This object is the first member of a new class

of cold telluric planets. Its detection confirms the power of this method and, given our detection efficiency, suggests that these recently-detected planets may be quite common around M stars, as confirmed by subsequent detection of a  $\sim 13$  Earth-mass planet. Using a network of dedicated 1–2-m-class telescopes, we have entered a new phase of planet discovery, and will be able to provide constraints on the abundance of frozen Super-Earths in the near future.

The discovery of extrasolar planets is arguably the most exciting development in astrophysics during the past decade, rivalled only by the discovery of the cosmic acceleration. The unexpected variety of giant exoplanets, some very close to their stars, many with high orbital eccentricity, has sparked a new generation of observers and theorists to address the question of how planets form in the context of protostellar accretion discs. Planets are now known to migrate and maybe even be ejected, via planet-disc and planet-planet interactions. We are beginning to discover how our Solar System fits into a broader community of planetary systems, many with very different properties. Microlensing-based searches play a critical role by probing for cool planets with masses down to that of Earth. Of key interest is how planets are distributed according to mass and orbital distance (Figure 1) as this information provides a crucial test for theories of planet formation. Core accretion models (Ida and Lin, 2005) are today the best description for the formation of planetary systems: the accretion of planetesimals leads to the formation of cores, which then start to accrete gas from the primitive nebula. This scenario predicts that for M dwarf stars there is a preferential formation of Earth- to Neptune-mass planets in 1–10 AU orbits. These planets are expected to form within a few million years. More massive planet (Jupiter) formation is hampered by a longer formation time (10 Myr) during which the gas evaporates and is no longer available to be accreted.

There is a wide variety of planets and at first sight it appears that our system is very special. However, our view of the whole picture is still blurred by observational biases inherent to the detection

techniques using transits and radial velocities. Both methods are more sensitive to massive planets close to their parent star. Doppler measurements and the space transit missions, such as COROT, can already, or will shortly, be able to detect Neptune-mass planets close to their parent star. Direct detections fill the other extreme of very large separations which are unknown in our Solar System. It is therefore necessary to use different techniques, each probing different areas of the planet-mass versus orbital distance parameter space.

Already with ground-based observations, the microlensing technique is sensitive to cool planets with masses down to that of the Earth orbiting 0.1–1  $M_{\odot}$  stars, the most common stars of our Galaxy, in orbits of 1–10 AU. Currently, over 700 microlensing events towards the Galactic Bulge are alerted in real time by the OGLE and MOA surveys each year. During these events, a source star is temporarily magnified by the gravitational potential of an intervening lens star passing near the line of sight, with an impact parameter smaller than the Einstein ring radius  $R_E$ , a quantity which depends on the mass of the lens, and the geometry of the alignment. For a source star in the Bulge, with a 0.3  $M_{\odot}$  lens,  $R_E \sim 2$  AU, the projected angular Einstein ring radius is  $\sim 1$  mas, and the time to transit  $R_E$  is typically 20–30 days, but can be in the range 5–100 days.

A planet orbiting the lens star generates a caustic structure in the source plane, with one small caustic around the centre of mass of the system, the central caustic, and one or two larger caustics further away, the planetary caustics. If the source star happens to reach the vicinity of one of the caustics, its magnification is significantly altered as compared to a single lens, resulting in a brief peak or dip in the observed light curve.

The duration of such planetary lensing anomalies scales with the square root of the planet's mass, lasting typically a few hours (for an Earth) to 2–3 days (for a Jupiter). These two caustics (Figure 2) provide two modes for detection. When the central caustic is approached for all events with a small impact angle between source and lens star, corresponding to a large peak magnification of the event,

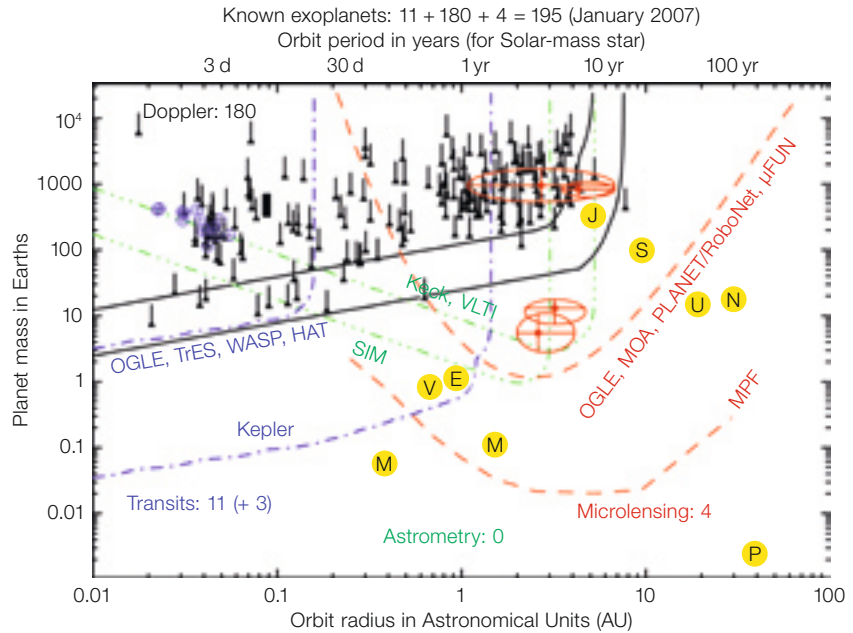
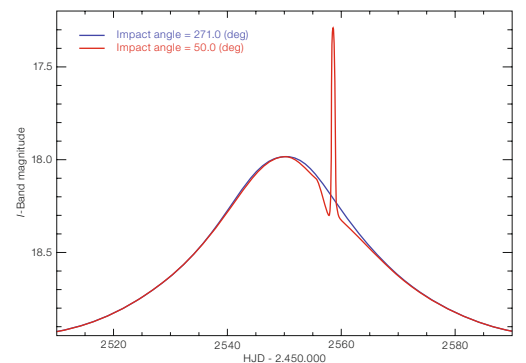
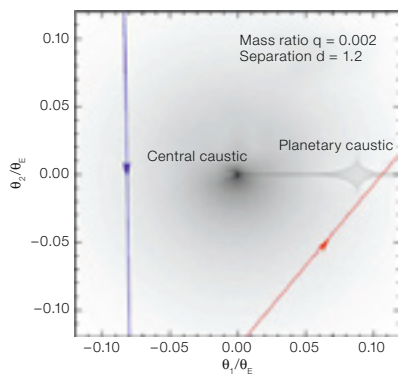


Figure 1 (above): Exoplanet discovery space (planet mass versus orbit size) showing the 8 planets from our Solar System (labelled as letters), 180 Doppler wobble planets (black triangles), 11 transit planets (blue circled crosses), and 4 microlensing planets (red circled crosses). Also outlined are the regions that can be probed by different methods: Doppler, transits; astrometry; and microlensing from the ground and space. Microlensing is a cost-efficient way to measure the mass function of cool planets down to the mass of the Earth.

Figure 2 (below): The left panel shows the caustic structure of a star/planet lens, with two possible trajectories of a source star. The right panel shows the corresponding observed light curves. Hitting the planetary caustic, or passing close to it, induces a short-lived but clearly detectable photometric signal.



the detection of planets in such events becomes highly efficient (Griest and Safizadeh 1998). In contrast, planetary caustics are only approached for a specific range of orientations of the source trajectory, but the characterisation of a planetary signal is much easier for such configurations.

The inverse problem, finding the properties of the lensing system, is a complex nonlinear one within a wide parameter

space to derive the planet/star mass ratio  $q$ , and the projected separation  $d$  in units of  $R_E$ . In general, model distributions for the spatial mass density of the Milky Way, the velocities of potential lens and source stars, and a mass function of the lens stars are required in order to derive probability distributions for the masses of the planet and the lens star, their distance, as well as the orbital radius and period of the planet, by means of Bayesian analysis.

The observational challenge is to monitor ongoing microlensing events, detected by the OGLE and MOA survey telescopes, with a fleet of telescopes to achieve round-the-clock monitoring and detect real-time deviations in the photometric signal. The telescopes belonging to our network together with their locations are shown in Figure 3. During the coming three Galactic Bulge seasons (from May to September 2007, 2008, 2009 in the southern hemisphere) we are planning to use the eight telescopes of the PLANET/RoboNET networks: Danish 1.5-m at La Silla (Chile), Canopus 1.0-m at Hobart and Bickley 0.6-m at Perth (Australia), Rockefeller 1.5-m at Bloemfontein and SAAO 1.0-m at Sutherland (South Africa). These are the standard telescopes of the PLANET network, to which were added in 2004 two robotic telescopes of the UK RoboNet network, North Faulkes 2-m in Hawaii and Liverpool 2-m in Canary islands, joined in 2006 by the South Faulkes 2-m in Australia.

### Observing strategy, and description of the reduction pipelines

A typical observing season of the Galactic Bulge starts at the beginning of May every year and lasts four months. Among the 691 alerts available in 2006 (579 from OGLE-III and 112 additional from MOA-II), about 180 are available every night in the middle of the season. Of these, around 20 targets can be monitored by 1-m-class telescopes, whereas the Danish 1.54-m and the 2-m telescopes can follow more events. Therefore, we must apply some criteria to select our 20 targets for every observing night. This is done by one member of the collaboration acting as a coordinator, the so-called 'homebase'. Depending upon the current magnification, the source brightness, and the time of the last observation, a priority algorithm assigns a worth to each of the events and suggests sampling rates, with the goal to maximise the planet detection efficiency. If the magnification of one event becomes very high, it may become the sole designated target during that night. While these suggestions are directly submitted to intelligent agents steering the robotic telescopes of the RoboNet network, the homebase currently tunes them using our experience gained, before



Figure 3: The different telescopes of the PLANET/RoboNet network.

instructing observers at the PLANET telescopes by means of a web page. We plan to embed our experience into future advanced versions of the priority algorithm and further automate this process.

At the beginning of the night, the observer finds on the PLANET web pages the list of targets with sampling intervals set up by the homebase. He then defines the exposure times for each target and reports them on our private web page, so that the homebase can estimate the observing load at each telescope. Typical sampling intervals are 0.5, 1, and 2 hours, according to the priority of each event. However, in case of a high magnification event, when the sensitivity to a planet is maximal, the sampling interval can be reduced to a few minutes, to the exclusion of all other candidate objects.

At the end of the exposure, the image is pre-processed (bias, dark removed and flatfielded), gets a standard name and is passed to an on-line pipeline. Starting in 2006, on all the PLANET telescopes, we shifted from a DoPhot-based on-line pipeline to an image subtraction pipeline based on ISIS (Alard 2000). This robust implementation, named WISIS, has two main tasks: *process* takes all available images of a given event, chooses the best template and subtracts all images from that template after convolving the reference point spread function (PSF) with the kernel to mimic the current PSF. The *update* task only processes new images using a previously chosen template.

In the case of OGLE, which has accumulated many images of a given field before a microlensing event is detected there, the template is built from a set of the best images and is not held fixed throughout the season. But in our case, we start observing an event when receiving the OGLE or MOA alert, so we have to build the template 'on the fly'. This generates problems when new images appear after a few nights, which are better than the first template. We then have to re-run the *process* routine on all images of the event. A different image subtraction pipeline is used on the RoboNet telescopes, but it follows the same philosophy.

The typical uncertainty of the on-line photometry is 1.2% for an  $I = 17.8$  mag Galactic Bulge star at the Danish 1.5-m telescope, and allows an on-line detection of a deviating signal. When this appears, excitement grows and an alert to homebase is issued. Homebase then prompts an off-line reduction of the event images, which are regularly uploaded to the Paris central archive. The off-line reduction is done with our other image subtraction pipeline, pySIS, which facilitates 'fine-tuning', so as to get the best possible photometry but is more difficult to automate for real-time use. If the off-line reduction confirms the deviation, an alert is issued to the microlensing community to intensify observations and maximise the chances of a good characterisation of the deviation, which is absolutely necessary for future modelling of the event. Moreover, all photometric data are made public immediately, as assistance to all teams in order to maximise the planet hunting community's success.

### The discovery of the frozen superEarth OGLE-2005-BLG-390Lb

On 11 July 2005, the OGLE Early Warning System announced the microlensing event OGLE 2005-BLG-390, with a relatively bright G4III giant as the source star. PLANET/RoboNet included it in its list of targets and started to monitor it on 25 July. The microlens peaked at a magnification  $A_{\max} = 3$  on 31 July. We were planning to continue to monitor it until the source exited the Einstein ring, when on 10 August observers at the Danish telescope noticed a measurement deviating

by 0.06 mag from the point source point lens prediction. They then took a second measurement, deviating by 0.12 mag. OGLE data became available, confirming the deviation seen in Chile. In order to check the nature of the deviation, home-base increased the proposed sampling rate at the automated Perth telescope. Perth started to observe this event continuously as soon as the target was within reach. South Africa was clouded out, and when observations resumed in Chile, it was clear that the anomaly was over. Different telescopes continued to observe the microlensing event. Perth data – which were received only with some delay – finally confirmed the short-duration deviation with a good coverage of six additional data points. Combined with two additional independent data points from the MOA team (Mt. John, New Zealand), the evidence of a well-covered short-term deviation from a point-lens light curve was on record (see Figure 4).

Frenetic modelling activities started and it became clear very quickly that we had discovered a low-mass planet. The analysis has proven to be rather straightforward for this event involving the transit of a large source star over a planetary caustic (Figure 5). The modelling of the photometric data yields the mass ratio  $q = 7.6 \pm 0.7 \cdot 10^{-5}$ , and the projected planet separation  $d = 1.61 \pm 0.008$  (in units of RE, the Einstein ring radius). We performed a Bayesian analysis using Galactic models and a mass function in order to derive probability distributions for the lens parameters (see Figure 2 from Beaulieu et al. 2006) and a constraint on the nature of the lens (low-mass main-sequence star or stellar remnant). The median values yield a host star of mass  $0.22^{+0.21}_{-0.11} M_{\odot}$  located at a distance of  $6.6 \pm 1.1$  kpc within the Galactic Bulge, orbited by a  $5.5^{+5.5}_{-2.7}$  Earth mass planet at an orbital separation of  $2.6^{+1.5}_{-0.6}$  AU (Figure 6, and the artist view of the planet by Herbert Zodet in ESO Press Release 02/06).

#### Planet detection efficiency

The detection efficiency of the experiment can be determined from all collected data, and comparison with the detections (or the absence of such) allows conclusions about the planet abundance

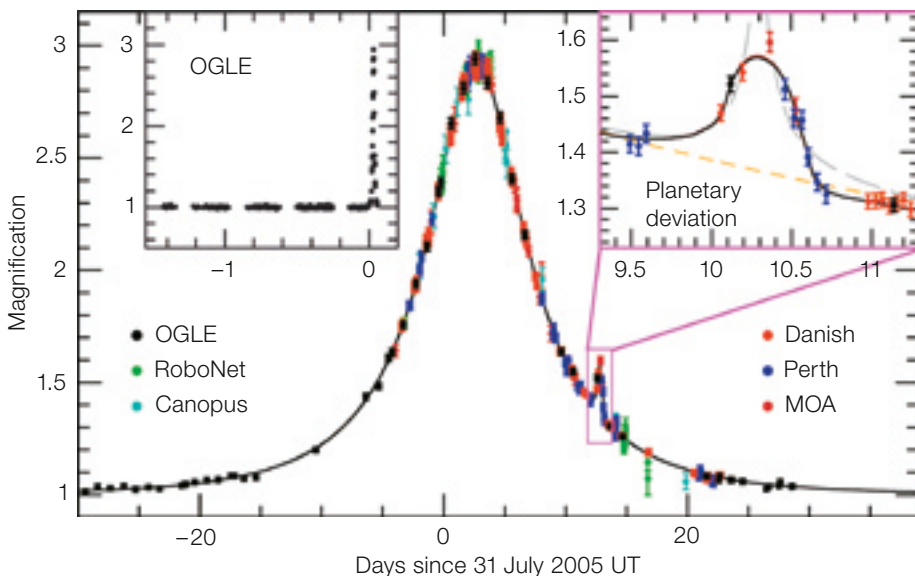


Figure 4: Light curve of OGLE-2005-BLG-390Lb, showing a brief planetary anomaly lasting for less than a day observed by four telescopes. The lens star is a  $\sim 0.22 M_{\odot}$  Galactic Bulge M dwarf orbited by a  $\sim 5.5$  Earth-mass planet at  $\sim 2.6$  AU with a

period of  $\sim 10$  years (plotted as solid line). The best alternative model is a binary source star but is rejected by the data. The dashed line is the point source point lens model without the planetary deviation (Beaulieu et al. 2006).

around the probed stars. The first attempts were done on individual high-magnification events using a point-source approximation, and then were applied to a sample of the 42 well-covered microlensing events acquired by PLANET in 1995–1999 (Gaudi et al. 2002). Less than 1/3 of the lenses are orbited by Jupiters with orbits in the range 1–5 AU. We are currently working on an analysis combining 11 years of data (1995–2005). We calculate the detection efficiency of each microlensing light curve to lensing companions as a function of the mass ratio and projected separation of the two components, now taking into account extended source effects. We use the same Bayesian analysis as for determining probability densities for the lens star and planet properties (Dominik 2006). Figure 7 gives the mean detection efficiency of PLANET combining 14 well-sampled events from 2004. For Jupiter-mass planets, the detection efficiency reaches 50%, while it decreases only with the square-root of the planet mass until the detection of planets is further suppressed by the finite size of the source stars for planets with a few Earth masses. Nevertheless, the detection efficiency still remains a few per cent for planets below 10 Earth masses, made of rock and ice. As of today, four planets have been de-

tected by microlensing, two of which are Jupiter analogues (Bond et al. 2004, Udalski et al. 2005) and one Neptune (Gould et al. 2006), where the perturbation is due to the central caustic, and one rocky/icy planet of 5.5 Earth mass named OGLE-2005-BLG-390Lb (Beaulieu et al., 2006) via a planetary caustic. They are overplotted on Figure 7. So the era of discovery of frozen Super-Earths has been opened by the microlensing technique. One of the consequences of the discovery of such a small planet, is that these small rock/ice planets should be common.

#### Obtaining more information about these planets

Unlike other techniques, microlensing does not offer much chance to study the planetary system in more detail because the phenomenon only occurs once for each star. Only a significant statistical sample will allow us to reach firm conclusions and finally answer the question of how special is our own Solar System. Additional information about a specific event can be obtained once the lens star is directly detected. Here, we must wait many years till the relative motion of the source and lens stars separate them on the sky.

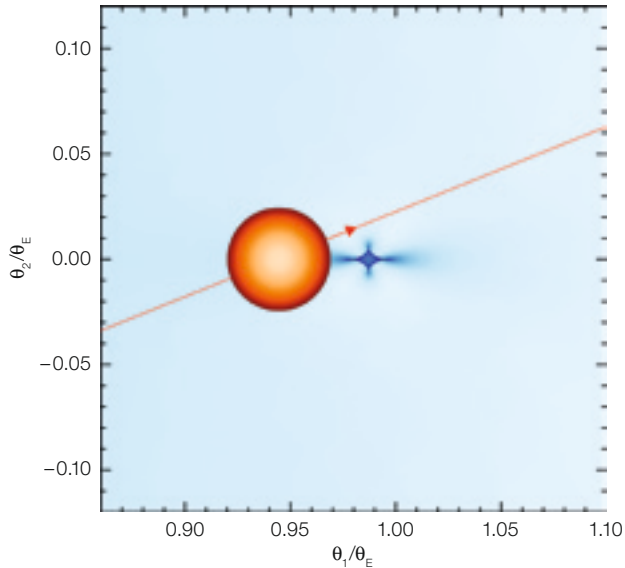


Figure 5: The source star and the planetary caustic of OGLE-2005-BLG6390. Notice the small size of the planetary caustic compared to the source star.

Bennett et al. (2006) using HST images have detected the lens star in the microlensing event OGLE-2003-BLG-235/MOA-2003-BLG-53, and therefore the uncertainty on the planetary parameters have been greatly reduced. This could be achieved too with HST or adaptive optics for OGLE-2005-BLG-169. In the case of the lens OGLE-2005-BLG-390La, the observation is much more difficult since we would need to detect a  $K \sim 22$  mag object at about 40 mas (in five years) from a star that is 10 mag brighter. In the coming years, statistics about frozen Super-Earth planets orbiting M and K dwarfs will be obtained, complementing the parameter space explored by space transit missions like COROT and KEPLER or aggressive ground-based Doppler search, like those using the CORALIE, SOPHIE and HARPS instruments.

#### Acknowledgements

Microlensing follow-up observations would not happen without the alert systems of the OGLE and MOA collaborations. We are very grateful to OGLE and MOA, and to the observatories that support our science (ESO, Canopus, CTIO, Perth, SAAO, Boyden) via the generous allocations of time that make this work possible. The operation of Canopus Observatory is in part supported by a financial contribution from David Warren, and the Danish telescope at La Silla is operated by IDA financed by SNF. The RoboNet project is funded by the UK STFC. HOLMES

is supported by the Agence Nationale de La Recherche. KHC work performed under auspices of US DOE, by UC, LLNL under contract, W 7405-Eng-48. NJR acknowledges financial support by a PPARC PDRA fellowship and is partially supported by the European Community's Sixth Framework Marie Curie Research Training Network Programme, Contract No. MRTN-CT-2004-505183 ANGLES.

#### References

- Alard C. 2000, A&AS 144, 363
- Beaulieu J. P. et al. 2006, Nature 439, 437
- Bennett D. P. et al. 2006, ApJ 647, 171
- Bond I. A. et al. 2005, ApJ 606, 155
- Dominik M. 2006, MNRAS 367, 669
- Gaudi B. S. et al. 2002, ApJ 566, 463
- Gould A. et al. 2006, ApJ 644, L 37
- Griest K. and Safizadeh N. 1998, ApJ 500, 37
- Ida S. and Lin D. N. C. 2005, ApJ 626, 1045
- Udalski A. et al. 2005, ApJ 628, 109

Figure 6: Perturbation of the image of the source star by the planetary caustic observed with an ideal telescope. The time interval between the images is 0.1 day. The image scale is 30 microarcsec (Bennett and Williams).

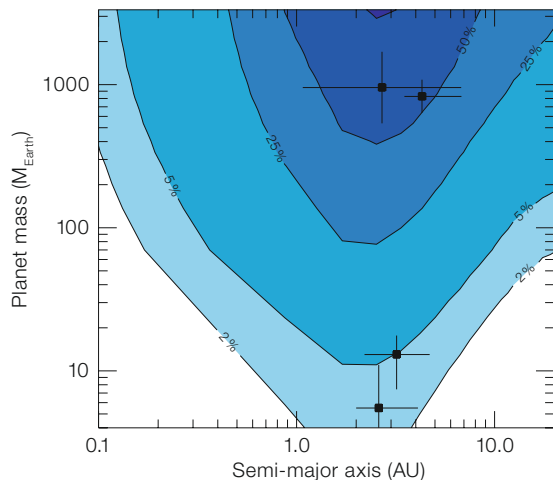
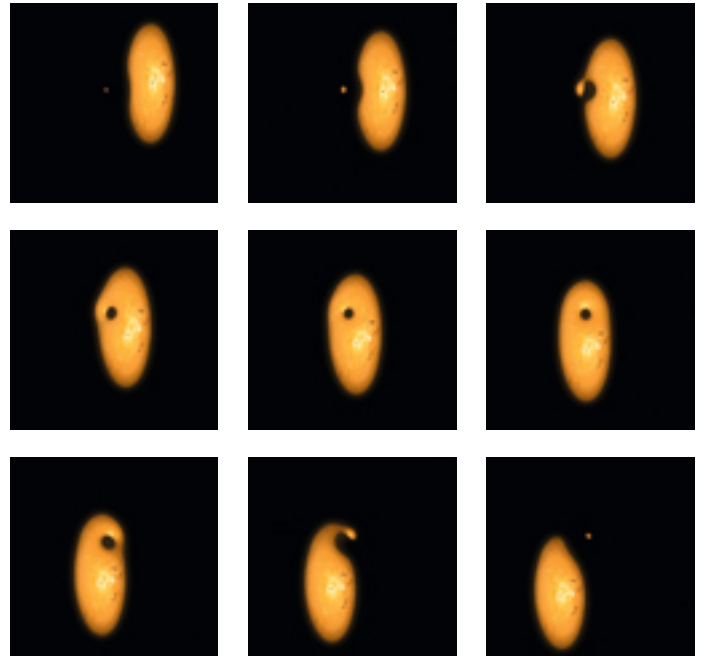


Figure 7: Average detection efficiency of planets as a function of mass and orbital separation (assuming circular orbits) in the 14 favourable events monitored by PLANET in 2004 (preliminary analysis) along with the planets detected by microlensing as of 2006 marked as points.

#### Relevant websites

- PLANET: <http://planet.iap.fr/>
- RoboNet: <http://www.astro.livjm.ac.uk/RoboNet/>
- MicroFUN: <http://www.astronomy.ohio-state.edu/~microfun/>
- MOA website: <http://www.phys.canterbury.ac.nz/moa/>
- OGLE website: <http://www.astrouw.edu.pl/~ogle/>